

## Mononuclear and Terminally Bound Titanium Nitrides

Maria E. Carroll, Balazs Pinter,<sup>†</sup> Patrick J. Carroll, and Daniel J. Mindiola\*

Department of Chemistry, University of Pennsylvania, 231 South 34th Street, Philadelphia, Pennsylvania 19104, United States

**S** Supporting Information

**ABSTRACT:** The Ti(III) azido complex  $(\text{PN})_2\text{Ti}(\text{N}_3)$  ( $\text{PN}^- = (N-(2-(\text{diisopropylphosphino})-4\text{-methylphenyl})-2,4,6\text{-trimethylanilide})$ ), can be reduced with  $\text{KC}_8$  to afford the nitride salt  $[\mu_2\text{-K}(\text{OEt}_2)]_2[(\text{PN})_2\text{Ti}\equiv\text{N}]_2$  in excellent yield. While treatment of the dimer with 18-crown-6 yields a mononuclear nitride, complete encapsulation of the alkali metal with cryptand provides the terminally bound nitride as a discrete salt  $[\text{K}(2,2,2\text{-Kryptofix})][(\text{PN})_2\text{Ti}\equiv\text{N}]$ . All complexes reported here have been structurally confirmed and also spectroscopically, and the Ti–N<sub>nitride</sub> bonding has been probed theoretically via DFT-based methods.

Titanium nitrides are an important class of molecules that are relevant to both heterogeneous and homogeneous chemistry. While titanium nitride films are of practical value in a variety of applications, including hydrodenitrogenation of oil feedstocks<sup>1</sup> and chemical vapor deposition methods,<sup>2</sup> molecular nitrides are fundamentally interesting given their proposed formation in a variety of reactions. As early as 1966, Vol'pin and Shur found that Ti(IV) complexes react with organo lithium and magnesium reagents under an atmosphere of  $\text{N}_2$  and upon treatment with acid, ammonia is formed.<sup>3</sup> Since that time, other titanium complexes were found to activate dinitrogen under reducing conditions and subsequently form ammonia and N-substituted organic compounds.<sup>4,5</sup> Molecular titanium nitrides are also proposed to be involved in cross-metathesis of alkylidynes with nitriles<sup>6</sup> and denitrogenation processes.<sup>7</sup>

Despite the wealth of examples of proposed titanium nitrides, well-defined exemplars of mononuclear titanium complexes having a terminally bound nitride ligand are unknown, similar to other group 4, as well as group 3, metals. The so-called “nitride-wall” can be attributed to the highly ionic nature of the polarized Ti–N multiple bond. As a result, terminally bound nitride ligands for titanium (or any group 4 metal) are unstable given their tendency to oligomerize.

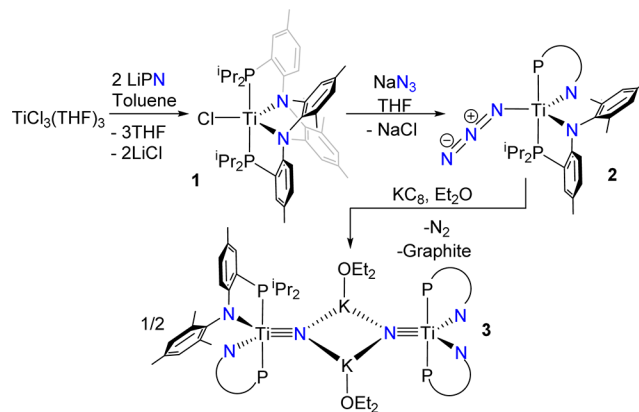
To alleviate the nucleophilic nature of the nitride ligand, Lancaster et al. have recently described various mononuclear titanium nitrides that are stabilized by Lewis acids, namely borane adducts.<sup>8–10</sup> Polynuclear titanium nitrides formed by ammonolysis of complexes of the type  $\text{L}_2\text{TiX}_2$  have also been reported,<sup>11–13</sup> however, in these cases, the nitride bridges three titanium centers. Also, Shima et al. have characterized a trititanium cluster containing a  $\mu_3$ -nitride ligand and a  $\mu_2$ -parent imido, where the nitrogenous ligands were derived from dinitrogen.<sup>14</sup> Similarly, the nitride  $\{[{}^i\text{Pr}_2\text{trenTi}]_2(\mu_3\text{-N})\text{Na}(\text{THF})\}$  ( ${}^i\text{Pr}_2\text{tren} = \text{N}(\text{CH}_2\text{CH}_2\text{N}^i\text{Pr}_2)_3$ ) can be prepared using  $\text{NaNH}_2$ .<sup>15</sup> Moreover, prior to 2014, there were only two examples of dinuclear titanium complexes containing  $\mu_2$ -nitride

ligands,<sup>16,17</sup> namely  $[\text{TiCl}_3\text{L}_2](\mu_2\text{-N})[\text{TiCl}_2\text{L}_3]$ , where L is 3,5-lutidine and  $\text{Na}_2[(\text{LTi})_2(\mu_2\text{-N})_2]$  ( $\text{L} = [(C_4H_3N)\text{-C}_6\text{H}_2]_2C_4H_2N(\text{Me})$ ).<sup>17</sup>

We recently described the synthesis and characterization of the titanium nitride dimer,  $[\mu_2\text{-K}]_2[{}^t\text{Bu}\text{-nacnac}]\text{Ti}\equiv\text{N}(\text{Ntoly}_2)_2$  ( ${}^t\text{Bu}\text{-nacnac}^- = [\text{ArNC}^t\text{Bu}]_2\text{CH}$ ;  $\text{Ar} = 2,6\text{-}^i\text{Pr}_2\text{C}_6\text{H}_3$ ), which served as a synthon for the corresponding mononuclear titanium nitride, when treated with various electrophiles.<sup>18</sup> Unfortunately, attempts to thoroughly study the Ti–N multiple bond in this species were hindered by the low solubility of the complex as well as the propensity of the nitride to decompose in polar solvents to intractable materials. To circumvent the vulnerability of the  $\beta$ -diketiminate ligand, we resorted to a more robust monoanionic chelating ligand  $\text{PN}^-$  ( $\text{PN}^- = (N-(2-(\text{diisopropylphosphino})-4\text{-methylphenyl})-2,4,6\text{-trimethylanilide})$ )<sup>19</sup> as well as explored a more direct route to this reactive functional group without the need to generate transient nitridyl species, which abstracted H• to form the parent imido  $[{}^t\text{Bu}\text{-nacnac}]\text{Ti}\equiv\text{NH}(\text{Ntoly}_2)$ .<sup>18</sup> Herein, we introduce a convenient entry to dinuclear and mononuclear titanium nitride complexes, as well as the isolation of the first discrete salt of titanium having a terminally bound nitride ligand.

When  $\text{TiCl}_3(\text{THF})_3$  is treated with 2 equiv of LiPN in toluene, complex  $(\text{PN})_2\text{TiCl}$  (**1**) is formed in 75% yield as orange-brown crystals (Scheme 1). Consistent with a paramagnetic,  $d^1$  complex, the  ${}^1\text{H}$  NMR spectrum of **1** features broadened chemical shifts ranging from 12 to  $-6$  ppm, and no signal for the PN ligand is observable in the  ${}^{31}\text{P}\{^1\text{H}\}$  NMR spectrum. The room-temperature Evans magnetic measurement in  $\text{C}_6\text{D}_6$  of **1** reveals a  $\mu_{\text{eff}}$

### Scheme 1. Synthesis of Complex 1 and the Titanium Nitride 3 by Reductive Denitrogenation of Azide 2



Received: May 10, 2015

Published: July 1, 2015

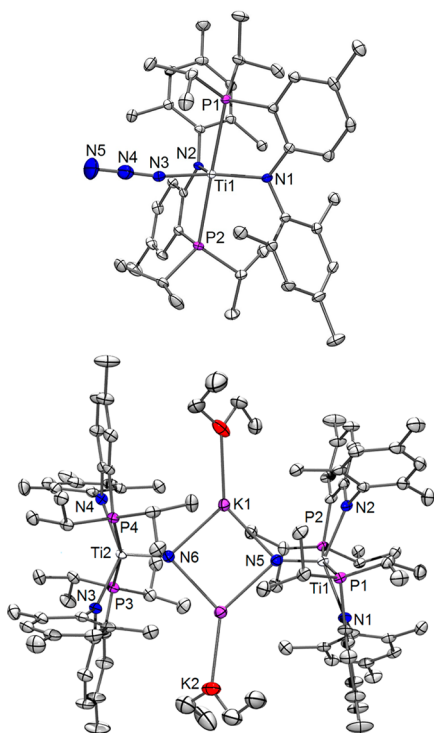


**Figure 1.** Molecular structures of compounds **2** (top) and **3** (bottom) showing thermal ellipsoids at the 50% probability level (with H atoms excluded). For **3**, toluene solvent molecules are omitted for clarity.

value of  $1.96 \mu_B$ , which is in accord with the spin-only  $\mu_{\text{eff}}$  value for an  $S = 1/2$  species. Single crystals of **1** were grown from a concentrated pentane solution that was cooled to  $-35^\circ\text{C}$ . A solid-state structure confirms the formation of a five-coordinate titanium(III) complex where the chloride ion occupies an equatorial position in a distorted trigonal bipyramidal geometry ( $\tau = 0.81$ ).<sup>20</sup> As a result, the phosphine residues of the PN ligands are transoid (P–Ti–P,  $178.957(16)^\circ$ ), occupying the axial sites.<sup>21</sup>

Treatment of **1** with a slight excess of  $\text{NaN}_3$  ( $\sim 1.2$  equiv) gives rise to the gradual formation of  $(\text{PN})_2\text{Ti}(\text{N}_3)$  (**2**) via the elimination of  $\text{NaCl}$ . Titanium(III) azide complexes are exceptionally rare, with the one other reported example being “ $\text{Cp}_2\text{TiN}_3$ ”, for which the only characterization tool was IR spectroscopy ( $\nu_{\text{N}_3} = 2050 \text{ cm}^{-1}$ ), owing to the unstable nature of such species.<sup>22</sup> Akin to **1**, complex **2** possesses one unpaired electron (Evans method  $\mu_{\text{eff}} = 1.92 \mu_B$ ,  $25^\circ\text{C}$ ,  $\text{C}_6\text{D}_6$ ) and should, accordingly, adopt a similar geometry to **1**, whereby the pseudo halide azide occupies an equatorial site. As shown in Figure 1, the solid-state structure confirms the proposed connectivity and geometry with a  $\tau$  value of 0.82 (P–Ti–P,  $178.957(16)^\circ$ ).

The IR spectrum of **2** in toluene shows a strong band at  $2104 \text{ cm}^{-1}$  and using  $\text{Na}^{15}\text{N}=\text{N}=\text{N}$ , affords a 50:50 mixture of  $(\text{PN})_2\text{Ti}^{15}\text{N}=\text{N}=\text{N}$  and  $(\text{PN})_2\text{TiN}=\text{N}=\text{N}^{15}\text{N}$ , as indicated by the appearance of two new bands of nearly equal intensity at  $2097$  and  $2089 \text{ cm}^{-1}$ .<sup>21</sup> Unlike transitory  $\beta$ -diketimate titanium(III) azides, which gradually convert to the parent imido, complex **2** is quite stable, with  $\text{C}_6\text{D}_6$  solutions being unchanged at room temperature for 24 h. Unfortunately, the exposure of **2** to more forcing conditions, such as heat or photolysis, resulted in the formation of multiple products, which we have been unable to purify or identify.

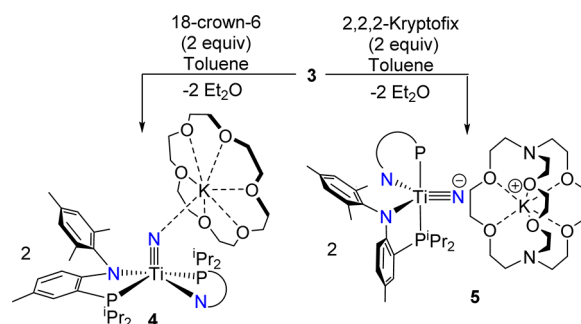
We hypothesized that one-electron reduction should promote  $\text{N}_2$  elimination to allow for direct entry to the nitride anion. Indeed, the progressive formation of a red-orange solid, concomitant with generation of graphite, was observed upon the treatment of **2** with  $\text{KC}_8$  in diethyl ether. Although the conversion  $\text{L}_n\text{M}^{\text{III}}\text{X} + \text{NaN}_3 \rightarrow \text{L}_n\text{M}^{\text{II}}\text{N} + \text{NaX} + \text{N}_2$  is a known occurrence, the formation of nitride salts directly from  $\text{NaN}_3$  takes place rather rarely.<sup>23,24</sup> Instances for azides-to-nitride reduction are also scarce and might actually suffer from competitive  $\text{N}_3^-$  salt elimination. For example, Brown and Peters have reported the bridging Fe nitride complex  $\text{Na}[\{\{\text{PhBP}_3\}\text{Fe}\}_2(\mu\text{-N})]$  ( $\text{PhBP}_3 = \text{PhB}(\text{CH}_2\text{PPh}_2)_3^-$ ), formed upon treatment of the dimeric iron azide complex  $\{\{\text{PhBP}_3\}\text{Fe}(\mu\text{-1,3-N}_3)\}_2$  with  $\text{Na}/\text{Hg}$ .<sup>25</sup>

Cooling a toluene solution of this new material layered with diethyl ether to  $-35^\circ\text{C}$  resulted in the formation of dark-orange crystals of a new diamagnetic species in 70% isolated yield. A solid-state structure analysis of a single crystal confirms the formation of a titanium nitride, where the  $\text{K}^+$  bridges each nitride to form the dimer  $[\mu\text{-K}(\text{OEt}_2)]_2[(\text{PN})_2\text{Ti}\equiv\text{N}]_2$  (**3**) (Figure 1). There is no symmetry element relating the two titanium fragments in the solid state, so the Ti– $\text{N}_{\text{nitride}}$  distances are different but very short at  $1.660(2)$  and  $1.674(2) \text{ \AA}$ . These distances are comparable to a similar species recently described by our group, namely  $[\text{K}]_2[(^t\text{Bu}^{\text{nacnac}})\text{Ti}\equiv\text{N}(\text{Ntoly})_2]_2$ .<sup>18</sup> Unlike the latter species, however, complex **3** does not exhibit any  $\text{K}^+\cdots\text{arene}$  interactions, but instead, the  $\text{K}^+$  ions adopt a three-coordinate and planar geometry as the result of each interacting to both nitrides and one  $\text{Et}_2\text{O}$  molecule. The K and  $\text{N}_{\text{nitride}}$  atoms form a planar diamond core (sum of four angles =  $360^\circ$ ), while the geometry at the Ti centers is intermediate between square pyramidal and trigonal bipyramidal ( $\tau = 0.52$ ).

Dimer **3** exhibits a higher symmetry in solution with a single signal in the  $^{31}\text{P}\{^1\text{H}\}$  NMR spectrum ( $\delta 7.2 \text{ ppm}$ ), indicating that all four phosphines of the PN ligands are in equivalent environments. Notably, the stability and reasonable solubility of **3** in aromatic solvents allowed us to collect reliable  $^{15}\text{N}$  NMR spectroscopic data and assign the highly downfield nitride resonance at  $892 \text{ ppm}$  (referenced versus  $\text{NH}_3(l)$  at  $0 \text{ ppm}$ ).

As noted before, the Ti-nitride functionality in compound **3** is remarkably stable, and thus the dimer can be broken by treatment with 2 equiv of 18-crown-6, to form the respective monomer  $[(\text{PN})_2\text{Ti}\equiv\text{NK}(18\text{-crown-6})]$  (**4**), in nearly quantitative yield (Scheme 2).  $^1\text{H}$  and  $^{31}\text{P}\{^1\text{H}\}$  NMR spectroscopic data are quite similar to **3**, while the  $^{15}\text{N}$  NMR spectrum for  $^{15}\text{N}$  enriched nitride **4** shows again a deshielded resonance at  $922 \text{ ppm}$ , a chemical shift that is  $\sim 30 \text{ ppm}$  further downfield relative to **3**. A solid-state structure of **4** also approves the monomeric

#### Scheme 2. Synthesis of the Mononuclear Titanium Nitride **4** and the Discrete Titanium Nitride Salt **5**



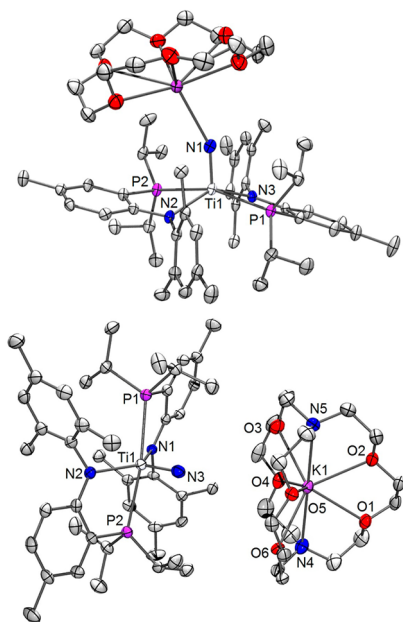


**Figure 2.** Molecular structures of compounds **4** (top) and **5** (bottom) showing thermal ellipsoids at the 50% probability level (with H atoms omitted). Solvent molecules are omitted for clarity.

form of the complex. The geometry around the titanium center in **4** is best described as distorted square pyramidal ( $\tau = 0.29$ ) with the nitride ligand occupying the apical site. Similar to **3**, the Ti–N<sub>nitride</sub> distance in **4** is short at 1.660(2) Å. The Ti–N–K angle is bent at 152.32(12)°, while the N<sub>nitride</sub>–K distance of 2.782(2) Å is slightly elongated compared to that in **3** with average N<sub>nitride</sub>–K distances of 2.734 Å. In all, the fairly small ring size of the crown ether leads to only partial encapsulation of the K<sup>+</sup> ion, so the nitride binds through the opposite side of the face of the [K(18-crown-6)]<sup>+</sup> component (top of Figure 2).

To completely encapsulate K<sup>+</sup> and form a discrete salt with a nitride ligand bound terminally to titanium, we resorted to the cryptand 4,7,13,16,21,24-hexaoxa-1,10-diazabicyclo[8.8.8]-hexacosane (2,2,2-Kryptofix). Treatment of **3** with this cryptand in toluene at –78 °C results in precipitation of an orange-brown colored solid in 90% yield. Crystallization of the solid from a THF solution layered with pentane at –35 °C provided single crystals of the discrete salt [K(2,2,2-Kryptofix)][(PN)<sub>2</sub>Ti≡N] (**5**), which was confirmed structurally by X-ray diffraction analysis (Scheme 2 and Figure 2). The K<sup>+</sup> cation no longer interacts with N<sub>nitride</sub> (~6.3 Å) in **5** due to its complete encapsulation by the cryptand. The geometry about the titanium center is best described as distorted trigonal bipyramidal ( $\tau = 0.66$ ), but interestingly, the Ti–N<sub>nitride</sub> bond distance is 1.719(3) Å, thus elongated compared to that of complexes **3** and **4** (vide infra). Unlike **3** and **4**, complex **5** is insoluble in nonpolar (aprotic) solvents. Compound **5** does, however, dissolve in tetrahydrofuran and dimethoxyethane, but these solvents react with it within minutes at room temperature, leading to a mixture of decomposition products, including K(PN). Overall, complex **5** displays similar spectroscopic features to **3** and **4**, including <sup>1</sup>H and <sup>31</sup>P{<sup>1</sup>H} NMR spectra that indicate, for example, one PN ligand environment. In order to slow down the decomposition process in THF-*d*<sub>8</sub>, a <sup>15</sup>N NMR of the <sup>15</sup>N-enriched nitride of **5** was collected at –80 °C. The <sup>15</sup>N NMR spectrum consists of an even further downfield shifted single resonance centered at 958 ppm.

**Table 1.** Experimental and Calculated Structural and Spectroscopic Properties of Monomeric Titanium Nitride Complexes **4** and **5**

	<b>4</b>	<b>5</b>
Ti–N <sub>Exp</sub> (Å)	1.660(2)	1.719(3)
Ti–N <sub>Calc</sub> (Å)	1.672	1.653
N–K <sub>Exp</sub> (Å)	2.782(2)	6.318(2)
N–K <sub>Calc</sub> (Å)	2.585	n/a <sup>a</sup>
<sup>15</sup> N NMR $\delta_{Exp}$ (ppm)	922.15	958.26
<sup>15</sup> N NMR $\delta_{Calc}$ (ppm)	907	946
Mulliken charges	Ti N	1.04 –0.87

<sup>a</sup>Complex **5** was modeled without the counterion K(2,2,2-Kryptofix)<sup>+</sup>.

To understand the bonding and <sup>15</sup>N NMR spectroscopic signature for this unique class of mononuclear nitride complexes, we modeled the structures of **4** (with K(18-crown-6)<sup>+</sup>) and **5** (without K(2,2,2-Kryptofix)<sup>+</sup>) using DFT methods.<sup>21</sup> The computed equilibrium structures reflect the observed characteristic features of mononuclear **4** and **5**, including their distorted square pyramidal and trigonal bipyramidal arrangements, respectively, as well as the computed structural metrics are in good overall agreement with the X-ray metrical parameters. Most importantly, the Ti–N<sub>nitride</sub> distance is excellently reproduced for **4** (Table 1), however it is underestimated by 0.06 Å for **5**. Such deviation most probably originates from omitting the K(2,2,2-Kryptofix)<sup>+</sup> counterion and other condensed phase effects in the simulations. The computed <sup>15</sup>N NMR chemical shifts also closely match those determined experimentally in solution, thus revealing strongly deshielded nitride nuclei in **4** and **5** and further implying that even the details of electronic structures are well reproduced *in silico*.

As presented in Figure 3, the MO analysis of **4** and **5**, carried out at the B3LYP/def2-TZVP level of theory, clearly reveals that the nitride ligand forms one  $\sigma$ -(1a<sub>1</sub>) and two  $\pi$ -type (1b<sub>1</sub> and 1b<sub>2</sub>) interactions to the titanium center, i.e., these species contain a formal Ti≡N functionality. Concomitantly with the computed MOs, a charge distribution analysis (Mulliken, Table 1) indicates that the overall Ti–N bonding is more covalent (Figure 3) in the terminal titanium nitride, **5**, than in **4** where the N<sup>3–</sup> ligand interacts with a K<sup>+</sup> ion (to formally form a [KN<sub>3</sub>]<sup>2–</sup> group). In other words, the Ti≡N functionality becomes highly polarized when approximated by K<sup>+</sup> compared to the hypothetical free N<sup>3–</sup>. Accordingly, the Ti center is more positive (by 0.2 *e*), and the N<sup>3–</sup> group is more negative (by 0.2 *e*) in **4** than in **5**. Within the MO framework, the proximity of K<sup>+</sup> to N<sup>3–</sup> manifests in lowering the energies of the N<sup>3–</sup> orbitals and, thus, creating a large disparity with the three corresponding titanium orbitals (*d*<sub>xz</sub>, *d*<sub>xy</sub>, *d*<sub>x<sup>2</sup>–y<sup>2</sup></sub>), as shown in Figure 3. Due to this energy mismatch the Ti–N bonding orbitals (1a<sub>1</sub>, 1b<sub>1</sub>, and 1b<sub>2</sub>) are augmented mostly with nitrogen character and, thus, make for a more ionic bond in **4**. In **5**, the energy difference between the N<sup>3–</sup> ligand and (PN)<sub>2</sub>Ti orbitals is smaller, resulting in better orbital overlap and thus Ti-nitride bonding orbitals that have more equal contributions from Ti and N. The experimentally observed shorter Ti–N<sub>nitride</sub> bond in **4** indicates that ion pairing with K<sup>+</sup>, beyond thermodynamically stabilizing **4**, also strengthens the terminal Ti–N<sub>nitride</sub> interaction. By means of protecting the Ti≡N functionality, K(18-crown-6)<sup>+</sup> also assigns a high kinetic stability to **4**, further corroborated given the observation that complex **4** is far more stable in solution than **5**.



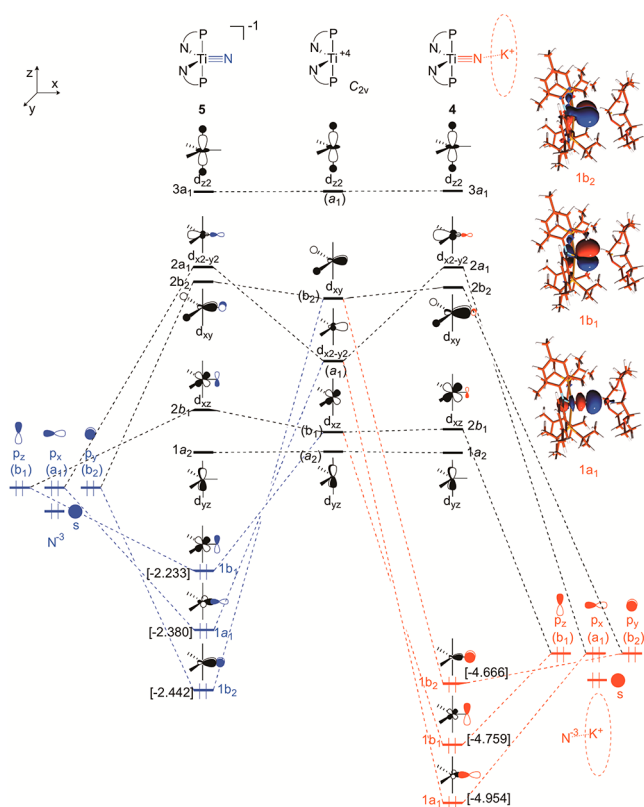


**Figure 3.** Schematic molecular orbital diagram for conceptualizing the difference in Ti–N<sub>nitride</sub> bonding in **4** (right) and **5** (left) and computed 1a<sub>1</sub>, 1b<sub>1</sub> and 1b<sub>2</sub> MOs of **4**, energies given in eV.

For this set of titanium nitride complexes, a downfield shift in the <sup>15</sup>N NMR resonances is observed on going from dimeric, **3**, to the monomeric, **4**, and to discrete nitride salt, **5**. As demonstrated, e.g., for terminal phosphides the paramagnetic shielding perpendicular to the M≡P bond significantly depends on the σ-HOMO–π-LUMO gap,<sup>28</sup> and accordingly, chemical shielding represents a footprint for the M≡X bonding. Our DFT calculations show that a more downfield chemical shift is associated with a decrease in the energy difference between the σ orbital of the Ti–N bond and the LUMO for the complex. This trend has been observed for a number of complexes containing transition metal–ligand triple bonds,<sup>26–28</sup> providing further justification of our description of the bonding in the present study as consisting of a Ti–N triple bond and its change upon K<sup>+</sup> coordination.

In conclusion, we have now expanded the “nitride wall” to group 4 transition metals, specifically to mononuclear and terminally bound titanium nitride salts. We break into this reactive ligand class by the reduction of a titanium-azide functionality. Our molecular orbital picture reveals the Ti≡N bonding in **4** to be more ionic, whereas for **5**, the encapsulation of the K<sup>+</sup> renders such interaction more covalent. We are presently examining the reactivity of this rare functional group on titanium as well as with other early transition metals.

## ■ ASSOCIATED CONTENT

### Supporting Information

Experimental procedures, spectral data, computational details, and crystallographic information (CIF). The Supporting Information is available free of charge on the ACS Publications website at DOI: 10.1021/jacs.5b04853.

## ■ AUTHOR INFORMATION

### Corresponding Author

\*mindiola@sas.upenn.edu

### Present Address

†Eenheid Algemene Chemie (ALGC), Vrije Universiteit Brussel, Pleinlaan 2, 1050 Brussels, Belgium.

### Notes

The authors declare no competing financial interest.

## ■ ACKNOWLEDGMENTS

This work was supported by the Chemical Sciences, Geosciences, and Biosciences Division, Office of Basic Energy Sciences, Office of Science, U.S. Department of Energy (DE-FG02-07ER15893).

## ■ REFERENCES

- (1) Furimsky, E.; Massoth, F. E. *Catal. Rev.: Sci. Eng.* **2005**, *47*, 297.
- (2) Weiller, B. H. *J. Am. Chem. Soc.* **1996**, *118*, 4975.
- (3) Vol'Pin, M. E.; Shur, V. B. *Nature* **1966**, *209*, 1236.
- (4) Van Tamelen, E. E. *Acc. Chem. Res.* **1970**, *3*, 361.
- (5) Mori, M. *Heterocycles* **2009**, *78*, 281.
- (6) Bailey, B. C.; Fout, A. R.; Fan, H.; Tomaszewski, J.; Huffman, J. C.; Gary, J. B.; Johnson, M. J. A.; Mindiola, D. J. *J. Am. Chem. Soc.* **2007**, *129*, 2234.
- (7) Fout, A. R.; Bailey, B. C.; Buck, D. M.; Fan, H.; Huffman, J. C.; Baik, M.-H.; Mindiola, D. J. *Organometallics* **2010**, *29*, 5409.
- (8) Fuller, A. M.; Hughes, D. L.; Jones, G. A.; Lancaster, S. J. *Dalton Trans.* **2012**, *41*, 5599.
- (9) Fuller, A. M.; Clegg, W.; Harrington, R. W.; Hughes, D. L.; Lancaster, S. J. *Chem. Commun.* **2008**, 5776.
- (10) Mountford, A. J.; Lancaster, S. J.; Coles, S. J. *Acta Crystallogr., Sect. C: Cryst. Struct. Commun.* **2007**, *63*, m401.
- (11) Gomez-Sal, P.; Martin, A.; Mena, M.; Yelamos, C. *J. Chem. Soc., Chem. Commun.* **1995**, 2185.
- (12) Abarca, A.; Gomez-Sal, P.; Martin, A.; Mena, M.; Poblet, J. M.; Yelamos, C. *Inorg. Chem.* **2000**, *39*, 642.
- (13) Roesky, H. W.; Bai, Y.; Noltemeyer, M. *Angew. Chem., Int. Ed. Engl.* **1989**, *28*, 754.
- (14) Shima, T.; Hu, S.; Luo, G.; Kang, X.; Luo, Y.; Hou, Z. *Science* **2013**, *340*, 1549.
- (15) Duan, Z.; Verkade, J. G. *Inorg. Chem.* **1996**, *35*, 5325.
- (16) Carmalt, C. J.; Mileham, J. D.; White, A. J. P.; Williams, D. J. *New J. Chem.* **2000**, *24*, 929.
- (17) Nikiforov, G. B.; Vidyaratne, I.; Gambarotta, S.; Korobkov, I. *Angew. Chem., Int. Ed.* **2009**, *48*, 7415.
- (18) Thompson, R.; Chen, C.-H.; Pink, M.; Wu, G.; Mindiola, D. J. *J. Am. Chem. Soc.* **2014**, *136*, 8197.
- (19) Tran, B. L.; Pink, M.; Mindiola, D. J. *Organometallics* **2009**, *28*, 2234.
- (20) Addison, A. W.; Rao, T. N.; Reedijk, J.; van Rijn, J.; Verschoor, G. C. *J. Chem. Soc., Dalton Trans.* **1984**, 1349.
- (21) See Supporting Information.
- (22) Coutts, R.; Wailes, P. C. *Inorg. Nucl. Chem. Lett.* **1967**, *3*, 1.
- (23) Brask, J. K.; Dura-Vila, V.; Diaconescu, P. L.; Cummins, C. C. *Chem. Commun.* **2002**, 902.
- (24) King, D. M.; Tuna, F.; McInnes, E. J. L.; McMaster, J.; Lewis, W.; Blake, A. J.; Liddle, S. T. *Nat. Chem.* **2013**, *5*, 482.
- (25) Brown, S. D.; Peters, J. C. *J. Am. Chem. Soc.* **2005**, *127*, 1913.
- (26) Sceats, E. L.; Figueroa, J. S.; Cummins, C. C.; Loening, N. M.; Van der Wel, P.; Griffin, R. G. *Polyhedron* **2004**, *23*, 2751.
- (27) Greco, J. B.; Peters, J. C.; Baker, T. A.; Davis, W. M.; Cummins, C. C.; Wu, G. *J. Am. Chem. Soc.* **2001**, *123*, 5003.
- (28) Wu, G.; Rovnyak, D.; Johnson, M. J. A.; Zanetti, N. C.; Musaev, D. G.; Morokuma, K.; Schrock, R. R.; Griffin, R. G.; Cummins, C. C. *J. Am. Chem. Soc.* **1996**, *118*, 10654.